

Received May 31, 2016, accepted June 8, 2016, date of publication June 14, 2016, date of current version July 7, 2016.

Digital Object Identifier 10.1109/ACCESS.2016.2580681

Wireless Information and Energy Transfer in Multi-Cluster MIMO Uplink Networks Through Opportunistic Interference Alignment

YUAN REN¹, TIEJUN LV¹, (Senior Member, IEEE), HUI GAO¹, (Member, IEEE),
AND SHAOSHI YANG², (Member, IEEE)

¹School of Information and Communication Engineering, Beijing University of Posts and Telecommunications, Beijing 100876, China

²School of Electronics and Computer Science, University of Southampton, Southampton SO17 1BJ, U.K.

Corresponding author: T. Lv (lvtiejun@bupt.edu.cn)

This work was supported in part by the National Natural Science Foundation of China under Grant 61401041 and Grant 61271188 and in part by the National High Technology Research and Development Program of China (863 Program) under Grant 2015AA01A706.

ABSTRACT In this paper, we consider a K -cluster ($K \geq 2$) simultaneous wireless information and power transfer network, where S nodes ($S \geq 2$) are selected from N nodes within each cluster for the uplink information transmission and the remaining $N - S$ idle nodes are dedicated to energy harvesting. Based on the intra-cluster performance aware (ICPA) philosophy, a pair of opportunistic interference alignment (OIA) schemes, namely, the coarse ICPA-OIA (C-ICPA-OIA) and the refined ICPA-OIA (R-ICPA-OIA), are proposed for balancing the sum rate performance achieved and the energy harvested. Specifically, the C-ICPA-OIA treats the overall signal strength within the reference signal subspace (RSS) as a coarse description of the node's effective signal strength. By comparison, to take full advantage of zero-forcing-based reception, the R-ICPA-OIA considers the projected signal strength with respect to the orthonormal basis of RSS as a substantially refined description of the node's effective signal strength. Furthermore, we analyzed the harvested power and the working time of the system. Extensive simulation results validate our theoretical analyses, demonstrating that our schemes outperform the existing OIA schemes.

INDEX TERMS Opportunistic interference alignment, multi-node scheduling, energy harvesting, simultaneous wireless information and power transfer.

I. INTRODUCTION

Interference alignment (IA), which was originally proposed for K -user/node interference channel [1], [2], has attracted considerable attention in recent years. The basic idea of IA is to align the interference imposed on the receiver into a subspace having lowest possible dimensions so that the interference-free dimensions can be maximized for the desired signal. IA has been studied in a variety of contexts, such as the single-cell or single-cluster multiple-input multiple-output (MIMO) interference channels [3] and multi-cell or multi-cluster networks [4], [5], showing a great potential for substantial performance improvement. Despite its merits predicted theoretically, IA faces many challenges in practical applications, such as the requirement of global channel state information (CSI) and a large number of signal dimensions, which are essential to the symbol/time/frequency expansion techniques invoked in the design of optimal IA transceivers. Owing to such unaffordable system overhead, limited feedback IA schemes [6]–[11] and distributed IA schemes [12] have been

proposed for mitigating the stringent CSI requirements. However, in order to achieve the full degrees-of-freedom (DoF), the number of bits required by the quantization of the feedback signal has to scale with the high transmission power in the limited feedback IA. Moreover, the computational complexity is prohibitive for the iterative calculation of the transmit/receive beamforming matrices in the distributed IA.

Furthermore, opportunistic interference alignment (OIA) has been proposed for both downlink [13]–[16] and uplink [17]–[23] transmissions in realistic multi-cell or multi-cluster systems. Compared with the traditional IA schemes [1]–[4], OIA enjoys many benefits. For example, it works well with local CSI, and it does not require symbol/time/frequency expansion or iterative calculation for beamforming. In the downlink OIA, the base stations broadcast random beamforming vectors to all users/nodes, and each user/node uses the chordal distance between the interfering channels as a performance metric to facilitate the user/node scheduling [13]. The achievable sum rate performance of the downlink OIA was further improved

in [14] by using a more-effective scheduling strategy. In the uplink OIA, the reference signal subspace (RSS) was employed to guide the transmission [17]–[23]. More specifically, in [17] and [18], an OIA scheme was proposed for the single-input multiple-output (SIMO) interfering multiple-access channel (IMAC) and the optimal DoF can be asymptotically achieved in the high signal-to-noise ratio (SNR) regime under proper user/node scaling conditions. The OIA was further extended to the MIMO IMAC scenario in [19], where a singular value decomposition (SVD) based joint transmit beamforming and user/node scheduling scheme was conceived. More recently, an active OIA scheme was proposed in [21], where the user/node scaling condition was relaxed and the DoF gain was achieved even with a small number of users/nodes. The user/node selection criteria were further improved in [21]–[24] by taking the intra-cell or intra-cluster performance into consideration, i.e., the useful signal strength and the leakage interference strength should be balanced for achieving higher sum rate.

In addition to wireless techniques offering high spectral efficiency (e. g. IA), green radio that aims for high energy efficiency has also become one of the key enabling technologies of the fifth generation (5G) wireless communication systems [25], which require extremely high data rate, ubiquitous coverage and potential power savings [26]. Wireless energy harvesting (EH) constitutes an important technique for achieving high energy efficiency promised by green radio [27], [28]. Since radio-frequency (RF) signals can be used as a vehicle for simultaneously transmitting information and energy, the scheme named simultaneous wireless information and power transfer (SWIPT) comes into being [29], [30]. In the traditional IA networks, the interference is considered harm to the system performance and should be eliminated, which is a great waste of energy from the view of EH. There are some initial contributions to the combination of IA and SWIPT in [27] and [28], which highlight the advantage of re-utilizing the interference for conducting EH. However, those contributions rely on the assumption that perfect IA is available, which restrains them from being extended to the classical OIA scenario [19], where perfect IA is not feasible.

In this paper, a pair of OIA schemes, which are termed the coarse intra-cluster performance aware OIA (C-ICPA-OIA) and the refined intra-cluster performance aware OIA (R-ICPA-OIA), respectively, are proposed for SWIPT systems. In particular, S N_r -antenna nodes ($S \geq 2$) are selected from N candidates ($N \geq S$) within each cluster and co-channel uplink transmission is carried out, while their N_r -antenna home cluster head (CH) employs a zero-forcing (ZF) receiver. During the uplink transmission, the $N - S$ unselected nodes harvest energy from the S selected nodes of each cluster. The scheduling metrics for the two ICPA-OIA schemes are designed to describe both the capability of information transmission (IT), which is characterized by the ratio of the desired signal strength to the interference strength, as well as the ability of EH, i.e., the amount

of energy provided by a node. More explicitly, the main contributions of this paper are summarized as follows.

- A pair of ICPA-OIA schemes are proposed for SWIPT systems to improve the EH performance, while maintaining the achievable sum rate performance. Different from the traditional OIA schemes [19], [31], our ICPA-OIA schemes consider both IT and EH simultaneously. Specifically, the C-ICPA-OIA takes the overall desired signal strength in the RSS of each node into consideration, while in the R-ICPA-OIA, both the intra-cluster performance and the leakage interference of the node is carefully measured. Compared with the conventional OIA schemes [19], [31], the proposed ICPA-OIA schemes are capable of harvesting a higher amount of energy. Moreover, the R-ICPA-OIA scheme also achieves higher sum rate than the conventional OIA schemes.
- The average harvested power by our ICPA-OIA schemes and by the two conventional node scheduling schemes [19], [31] are analyzed, which verifies the advantages of the proposed schemes. Furthermore, the working time of the system invoking different OIA schemes are provided to show the EH performance of the proposed schemes.
- The computational complexity of the proposed ICPA-OIA schemes and of the traditional OIA schemes [19], [31] is studied, which demonstrates that the proposed schemes impose a comparable computational complexity to the traditional OIA schemes. A reduced-feedback design is also proposed for R-ICPA-OIA.

The remainder of this paper is organized as follows. Our system model is described in Section II. ICPA-OIA schemes proposed for SWIPT systems are detailed in Section III. We analyze the performance of the proposed ICPA-OIA schemes in Section IV. Numerical results and discussions are provided in Section V. Finally, our conclusions are drawn in Section VI.

Notations: We use uppercase boldface letters for matrices and lowercase boldface for vectors. $(\cdot)^T$, $(\cdot)^H$, $(\cdot)^\dagger$, $\|\cdot\|$ and $E[\cdot]$ denote the transpose, conjugate transpose, pseudo-inverse, Euclidean-norm and expectation, respectively. $\lambda_n(\mathbf{A})$ and $\mathbf{w}_n(\mathbf{A})$ denote the n -th largest eigenvalue and the eigenvector corresponding to $\lambda_n(\mathbf{A})$, respectively. $\lambda_n(\mathbf{A}, \mathbf{B})$ and $\mathbf{w}_n(\mathbf{A}, \mathbf{B})$ denote the n -th largest generalized eigenvalue and the generalized eigenvector corresponding to $\lambda_n(\mathbf{A}, \mathbf{B})$, respectively. \mathbb{C} represents the set of complex numbers. $\mathcal{CN}(\mu, \sigma^2)$ denotes a complex-valued Gaussian variable with mean μ and variance σ^2 . The integer set $\{1, 2, \dots, K\}$ is abbreviated as $[1, K]$.

II. SYSTEM MODEL

As depicted in Fig. 1, we consider a K -cluster time-division duplex (TDD) uplink interference network, where each cluster consists of an N_r -antenna CH and $N(N \geq N_r)$ N_r -antenna nodes. The node set in cluster k is denoted by

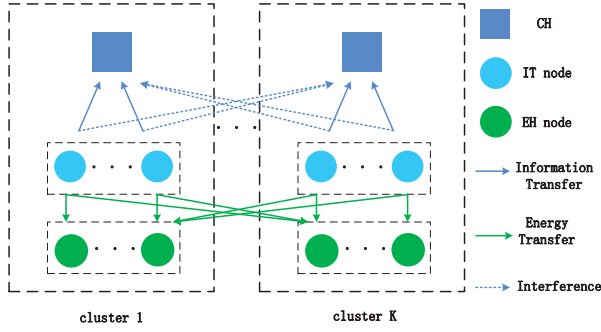


Fig. 1. The system model considered: K -cluster uplink interference network, where each cluster has one N_r -antenna CH and N_t N_t -antenna nodes. For the cluster k , S nodes, i.e., $\{D_{k,\psi_k(1)}, \dots, D_{k,\psi_k(S)}\}$, are selected for uplink transmission and the unselected $N - S$ nodes, i.e., $\{D_{k,\varphi_k(1)}, \dots, D_{k,\varphi_k(N-S)}\}$ harvest energy from the selected nodes in each cluster, where $k \in [1, K]$.

$\Omega_k = \{D_{k,1}, D_{k,2}, \dots, D_{k,N}\}$, $k \in [1, K]$. During each transmission block, S nodes¹ are selected to conduct S single-stream uplink transmissions in each cluster and the $N - S$ unselected nodes are dedicated to EH with the energy being harvested from the S selected nodes in each cluster, where we have² $2 \leq S \leq N_r < KS$. In the considered network, the IT receiver and the EH receiver are geographically separated. The indices of the selected and unselected nodes in cluster k are denoted by $\Psi_k = \{\psi_k(1), \dots, \psi_k(S)\}$ and $\Phi_k = \{\varphi_k(1), \dots, \varphi_k(N - S)\}$, respectively. For $k \in [1, K]$, we have $\Psi_k = [1, N] - \Phi_k$.

As far as IT is concerned, we denote the $(N_r \times N_t)$ -dimensional channel matrix from $D_{k,j}$ to CH_k as $\mathbf{H}_{k,j}^{[s]} = \beta_{k,j}^{[s]} \mathbf{G}_{k,j}^{[s]}$, $j \in \Psi_k$ and $s, k \in [1, K]$. $\mathbf{G}_{k,j}^{[s]} \in \mathbb{C}^{N_r \times N_t}$ is the small-scale fading channel matrix from $D_{k,j}$ to CH_k , $\beta_{k,j}^{[s]}$ is the distance-dependent path-loss coefficient of the channel from $D_{k,j}$ to CH_k . On the other hand, for EH, we denote the $(N_t \times N_t)$ -dimensional channel matrix from $D_{p,j}$ to $D_{k,i}$ as $\mathbf{H}_{p,j}^{[k,i]} = \beta_{p,j}^{[k,i]} \mathbf{G}_{p,j}^{[k,i]}$, $j \in \Psi_p$, $i \in \Phi_k$ and $p, k \in [1, K]$. $\mathbf{G}_{p,j}^{[k,i]} \in \mathbb{C}^{N_t \times N_t}$ is the small-scale fading channel matrix from $D_{p,j}$ to $D_{k,i}$, $\beta_{p,j}^{[k,i]}$ is the distance-dependent path-loss coefficient of the channel from $D_{p,j}$ to $D_{k,i}$. $\mathbf{G}_{p,j}^{[s]}$ and $\mathbf{G}_{p,j}^{[k,i]}$ are assumed to be independent and identically distributed (i.i.d.) Rayleigh block fading channels. Hence, each entry of $\mathbf{G}_{p,j}^{[s]}$ and $\mathbf{G}_{p,j}^{[k,i]}$ obeys $\mathcal{CN}(0, \sigma_1^2)$ and $\mathcal{CN}(0, \sigma_2^2)$, respectively. We assume that local CSI is known to each node, i.e., CH_k knows the path-loss coefficient and the small-scale fading CSI from the N nodes Ω_k , while $D_{k,j}$ knows the path-loss coefficient and the small-scale fading CSI from all the K CHs and the $N - 1$ nodes $\Omega_k - \{D_{k,j}\}$.

Before conducting the node selection, each CH will generate its RSS and broadcast it to all the nodes in

¹As shown in [19], the optimal value of S is $S = 1$, especially in the high-SNR regime. In this paper, we mainly focus on a multi-node transmission scenario. Therefore, $S \geq 2$ is assumed.

²If $N_r \geq KS$, the maximum DoF can be achieved in each cluster by employing the conventional ZF receiver at CH_k .

the network. Specifically, CH_i randomly generates an $N_r \times N_r$ unitary matrix $\mathbf{Q}^{[i]}$ and divides the matrix into two parts, i.e. the interference subspace (IS) $\mathbf{T}^{[i]}$ and the RSS $\mathbf{U}^{[i]}$. $\mathbf{T}^{[i]} = [\mathbf{t}_1^{[i]}, \dots, \mathbf{t}_{N_r-S}^{[i]}] \in \mathbb{C}^{N_r \times (N_r-S)}$, where $\mathbf{t}_p^{[i]} \in \mathbb{C}^{N_r \times 1}$, $i \in [1, K]$, $p \in [1, N_r - S]$, is formed by arbitrary $N_r - S$ columns of $\mathbf{Q}^{[i]}$; and $\mathbf{U}^{[i]} = [\mathbf{u}_1^{[i]}, \dots, \mathbf{u}_S^{[i]}] \in \mathbb{C}^{N_r \times S}$, where $\mathbf{u}_q^{[i]} \in \mathbb{C}^{N_r \times 1}$, $i \in [1, K]$, $q \in [1, S]$, is formed by the rest S columns of $\mathbf{Q}^{[i]}$. From the view of CH_i , $\mathbf{U}^{[i]}$ is used for measuring the leakage interference of all the nodes in other clusters, which also indicates how closely the channels of the nodes in other clusters are aligned with the span of $\mathbf{T}^{[i]}$. If $N_r = S$, then $\mathbf{U}^{[i]} = \mathbf{Q}^{[i]}$, which means the entire signal space is invoked to transmit data and the RSS of CH_i becomes a unitary matrix.

A. BASIC OIA TRANSMISSION SCHEME

The basic procedure of the uplink OIA scheme mainly includes five steps during each transmission block. 1) CH_i randomly generates its RSS, and broadcasts it to all the nodes in the network.³ 2) According to a certain selection criterion that is detailed later, each node calculates its scheduling metric and feeds it back to its home CH. 3) Each CH selects S nodes based on the feedback metrics and broadcasts the scheduling information to its nodes. 4) The selected nodes transmit data to its CH and the unselected nodes harvest energy from the selected nodes in each cluster. 5) Each CH detects the received signals using a simple ZF receiver.

The received signal $\mathbf{y}_k \in \mathbb{C}^{N_r \times 1}$ at CH_k is expressed as

$$\mathbf{y}_k = \sum_{s=1}^S \mathbf{H}_{k,\psi_k(s)}^{[k]} \mathbf{v}_{k,\psi_k(s)} x_{k,\psi_k(s)} + \sum_{i=1, i \neq k}^K \sum_{j=1}^S \mathbf{H}_{i,\psi_i(j)}^{[k]} \mathbf{v}_{i,\psi_i(j)} x_{i,\psi_i(j)} + \mathbf{n}_k, \quad (1)$$

where $x_{k,\psi_k(s)}$ is a single symbol simultaneously transmitted on all N_t transmit antennas of $D_{k,\psi_k(s)}$, $\mathbf{v}_{k,\psi_k(s)}$ denotes the transmit beamforming vector of $D_{k,\psi_k(s)}$, and $\mathbf{n}_k \in \mathbb{C}^{N_r \times 1}$ denotes the additive white Gaussian noise (AWGN) vector with its elements obeying i.i.d. $\mathcal{CN}(0, \sigma^2)$. It is assumed that the maximum transmit power is P_t , i.e., $\mathbb{E}[|x_{k,\psi_k(s)}|^2] \leq P_t$. The ZF receiver invoked to recover the transmitted signal is characterized as follows:

$$\bar{\mathbf{x}}_{k,\psi_k(s)} = [x_{k,\psi_k(1)}, \dots, x_{k,\psi_k(S)}]^T = \mathbf{G}^{[k]} \mathbf{U}^{[k]H} \mathbf{y}_k, \quad (2)$$

where $\mathbf{G}^{[k]} = [\bar{\mathbf{h}}_{k,\psi_k(1)}^{[k]}, \dots, \bar{\mathbf{h}}_{k,\psi_k(S)}^{[k]}]^\dagger \in \mathbb{C}^{S \times S}$ and $\bar{\mathbf{h}}_{k,\psi_k(s)}^{[i]} = \mathbf{U}^{[i]H} \mathbf{H}_{k,\psi_k(s)}^{[i]} \mathbf{v}_{k,\psi_k(s)} \in \mathbb{C}^{S \times 1}$ is the equivalent channel vector from $D_{k,\psi_k(s)}$ to CH_i . The instantaneous signal-to-interference-plus-noise ratio (SINR) of $D_{k,\psi_k(s)}$ is

³Alternatively, the RSS and IS can be determined offline and hence known to all the nodes in the system before the uplink data transmission takes place.

formulated as

$$\text{SINR}_{k,\psi_k(s)} = \frac{\rho}{\rho \sum_{i=1, i \neq k}^K \sum_{j=1}^S \left| \mathbf{g}_s^{[k]T} \tilde{\mathbf{h}}_{i,\psi_i(j)}^{[k]} \right|^2 + \left\| \mathbf{g}_s^{[k]} \right\|^2}, \quad (3)$$

where $\mathbf{g}_s^{[k]} \in \mathbb{C}^{S \times 1}$ is the s -th column of $\mathbf{G}^{[k]}$ and ρ is the transmit signal-to-noise ratio (SNR). Then, the instantaneously achievable sum rate of the network is given by

$$R_{\text{sum}} = \sum_{k=1}^K \sum_{s=1}^S \log(1 + \text{SINR}_{k,\psi_k(s)}). \quad (4)$$

B. WIRELESS POWER TRANSFER

Inspired by the idea of [27], when the selected nodes $\{D_{p,\psi_p(s)}\}$, $s \in [1, S]$, transmit data to its CH, the unselected nodes $\{D_{k,\varphi_k(n)}\}$, $n \in [1, N - S]$, are capable of harvesting power from the selected nodes $\{D_{p,\psi_p(s)}\}$, $s \in [1, S]$, and recharging their batteries. The received signal of the unselected nodes $D_{k,\varphi_k(n)}$ can be expressed as

$$\mathbf{y}_{k,\varphi_k(n)} = \sum_{p=1}^K \sum_{s=1}^S \mathbf{H}_{p,\psi_p(s)}^{[k,\varphi_k(n)]} \mathbf{v}_{p,\psi_p(s)} x_{p,\psi_p(s)} + \mathbf{n}_{k,\varphi_k(n)}, \quad (5)$$

where $\mathbf{n}_{k,\varphi_k(n)} \in \mathbb{C}^{N_t \times 1}$ is AWGN noise at $D_{k,\varphi_k(n)}$. According to [29], the energy harvested from the background noise can be ignored. Therefore, the harvested power at $D_{k,\varphi_k(n)}$ can be quantified as

$$\begin{aligned} Q_{k,\varphi_k(n)} &= \zeta \sum_{p=1}^K \sum_{s=1}^S \left\| \mathbf{H}_{p,\psi_p(s)}^{[k,\varphi_k(n)]} \mathbf{v}_{p,\psi_p(s)} x_{p,\psi_p(s)} \right\|^2 \\ &= \zeta P_t \sum_{p=1}^K \sum_{s=1}^S \left\| \tilde{\mathbf{h}}_{p,\psi_p(s)}^{[\varphi_k(n)]} \right\|^2, \end{aligned} \quad (6)$$

where ζ is a constant representing the energy conversion efficiency imposed by the energy transducer for converting the harvested energy to electrical energy and $\tilde{\mathbf{h}}_{p,\psi_p(s)}^{[\varphi_k(n)]} = \mathbf{H}_{p,\psi_p(s)}^{[k,\varphi_k(n)]} \mathbf{v}_{p,\psi_p(s)}$ is the equivalent channel vector from $D_{p,\psi_p(s)}$ to $D_{k,\varphi_k(n)}$. The sum of the harvested power in the network is given by

$$\bar{Q}_{\text{sum}} = \sum_{k=1}^K \sum_{n=1}^{N-S} Q_{k,\varphi_k(n)}. \quad (7)$$

C. CONVENTIONAL NODE SCHEDULING SCHEMES

In order to clarify the motivation for our new OIA schemes, two representative conventional opportunistic user/node scheduling schemes, i.e., the minimizing leakage interference (Min-LIF) based scheme [19] and the threshold based scheme [31] are briefly reviewed as follows.

1) MIN-LIF BASED USER/NODE SCHEDULING

The scheduling metric of $D_{k,j}$ is defined as

$$M_{k,j}^{\text{Min-LIF}} = \sum_{i=1, i \neq k}^K \left\| \mathbf{U}^{[i]H} \mathbf{H}_{k,j}^{[i]} \mathbf{v}_{k,j} \right\|^2. \quad (8)$$

The Min-LIF based node scheduling is an altruistic node selection scheme, where S nodes are selected in each cluster to minimize the interference generated to the other clusters, i.e., to minimize the leakage interference. The optimal transmit beamforming vector is

$$\mathbf{v}_{k,j}^{\text{Min-LIF}} = \arg \min_{\mathbf{v}_{k,j}} \left\| \tilde{\mathbf{G}}_{k,j} \mathbf{v}_{k,j} \right\|^2 = \mathbf{w}_{N_t} \left(\tilde{\mathbf{G}}_{k,j}^H \tilde{\mathbf{G}}_{k,j} \right), \quad (9)$$

where

$$\begin{aligned} \tilde{\mathbf{G}}_{k,j} &= [(\mathbf{U}^{[1]H} \mathbf{H}_{k,j}^{[1]})^T, \dots, (\mathbf{U}^{[k-1]H} \mathbf{H}_{k,j}^{[k-1]})^T, \\ &\quad (\mathbf{U}^{[k+1]H} \mathbf{H}_{k,j}^{[k+1]})^T, \dots, (\mathbf{U}^{[K]H} \mathbf{H}_{k,j}^{[K]})^T]^T, \end{aligned}$$

is the total cross-link channel matrix and $\mathbf{w}_n(\mathbf{A})$ denotes the eigenvector corresponding to the n -th largest eigenvalue of \mathbf{A} . Although the Min-LIF based OIA aims for mitigating the inter-cluster interference to ensure the achievability of the full DoF, it neglects the useful signal strength within the cluster, which may potentially be exploited for better performance.

2) THRESHOLD BASED USER/NODE SCHEDULING

The Min-LIF node scheduling scheme is designed relying on minimizing the total LIF for the sake of achieving the full DoF of the system. Therefore, the optimum sum rate performance of the system cannot be guaranteed by the Min-LIF scheme, especially in the low-to-medium SNR regime. Inspired by this observation, a threshold based node scheduling scheme was proposed in [31], which considers both the leakage interference and the desired signal strength. In the threshold based node scheduling, N_r nodes are selected in each cluster. For a certain receive beamforming vector $\mathbf{u}_m^{[k]}$, $k \in [1, K]$, $m \in [1, \dots, N_r]$, $D_{k,j}$ generates its transmit beamforming vector to minimize both the intra-cluster and the inter-cluster interference. Then, $D_{k,j}$ checks the following two conditions for each m and finds $m^* \in \{1, \dots, N_r\}$ that satisfies the following criteria

$$\begin{aligned} & \left| \mathbf{u}_{m^*}^{[k]H} \mathbf{H}_{k,j}^{[k]} \mathbf{v}_{k,j} \right|^2 \geq \eta_{tr}, \quad (10) \\ & \sum_{m=1, m \neq m^*}^{N_r} \left| \mathbf{u}_m^{[k]H} \mathbf{H}_{k,j}^{[k]} \mathbf{v}_{k,j} \right|^2 \\ & + \sum_{i=1, i \neq k}^K \sum_{m=1}^{N_r} \left| \mathbf{u}_m^{[i]H} \mathbf{H}_{k,j}^{[i]} \mathbf{v}_{k,j} \right|^2 \leq \eta_l, \quad (11) \end{aligned}$$

where η_{tr} and η_l represent the threshold values of the desired signal power and the total LIF, respectively. The optimal transmit beamforming vector is

$$\mathbf{v}_{k,j}^{\text{Threshold}} = \arg \min_{\mathbf{v}_{k,j}} \left\| \tilde{\mathbf{G}}_{k,j} \mathbf{v}_{k,j} \right\|^2 = \mathbf{w}_{N_t} \left(\tilde{\mathbf{G}}_{k,j}^H \tilde{\mathbf{G}}_{k,j} \right), \quad (12)$$

where $\tilde{\mathbf{G}}_{k,j} = \left[\left(\mathbf{U}_{m^*}^{[k]H} \mathbf{H}_{k,j}^{[k]} \right)^T, \tilde{\mathbf{G}}_{k,j}^T \right]^T$ and $\mathbf{U}_{m^*}^{[k]} = \left[\mathbf{u}_1^{[k]}, \dots, \mathbf{u}_{m^*-1}^{[k]}, \mathbf{u}_{m^*+1}^{[k]}, \dots, \mathbf{u}_{N_r}^{[k]} \right]$. As shown in [31], the sum rate performance of the threshold based scheme outperforms the Min-LIF scheme. However, in the threshold based scheme, the transmit beamforming vector was designed only

for minimizing the total LIF rather than for boosting the desired signal strength simultaneously. Moreover, neither of the two node scheduling schemes considered EH in the scheduling metric design. Therefore, they cannot be directly extended to the SWIPT based green communication systems.

III. THE PROPOSED OIA SCHEMES FOR SWIPT NETWORK

In this section, we propose a pair of OIA schemes for the SWIPT network, in which both node selection algorithm and the transmit beamforming vectors employed at the selected nodes are carefully designed to enhance the sum rate performance and the harvested power simultaneously.

A. THE PROPOSED SCHEME I: C-ICPA-OIA

In the traditional OIA schemes, the scheduling metrics are designed to improve the system's sum rate performance through minimizing the leakage interference and/or maximizing the desired signal strength. In order to jointly optimize both the sum rate and the harvested power in the network, new scheduling metric has to be designed. In this subsection, a C-ICPA-OIA scheme is proposed for characterizing both the IT and EH performance.

The scheduling metric for $D_{k,j}$ is defined as

$$\begin{aligned}
 M_{k,j}^C &= \frac{\alpha_{k,j} \left\| \mathbf{U}^{[k]H} \mathbf{H}_{k,j}^{[k]} \mathbf{v}_{k,j} \right\|^2 + (1 - \alpha_{k,j}) \zeta \sum_{i \neq j}^N \left\| \mathbf{H}_{k,j}^{[k,i]} \mathbf{v}_{k,j} \right\|^2}{\sum_{i=1, i \neq k}^K \left\| \mathbf{U}^{[i]H} \mathbf{H}_{k,j}^{[i]} \mathbf{v}_{k,j} \right\|^2} \\
 &= \frac{\mathbf{v}_{k,j}^H \mathbf{B}_{k,j} \mathbf{v}_{k,j}}{\mathbf{v}_{k,j}^H \mathbf{A}_{k,j} \mathbf{v}_{k,j}}, \tag{13}
 \end{aligned}$$

where we have

$$\begin{aligned}
 \mathbf{B}_{k,j} &= \alpha_{k,j} \mathbf{H}_{k,j}^{[k]H} \mathbf{U}^{[k]} \mathbf{U}^{[k]H} \mathbf{H}_{k,j}^{[k]} \\
 &+ (1 - \alpha_{k,j}) \zeta \sum_{i=1, i \neq j}^N \mathbf{H}_{k,j}^{[k,i]H} \mathbf{H}_{k,j}^{[k,i]}, \tag{14}
 \end{aligned}$$

$$\mathbf{A}_{k,j} = \sum_{i=1, i \neq k}^K \mathbf{H}_{k,j}^{[i]H} \mathbf{U}^{[i]} \mathbf{U}^{[i]H} \mathbf{H}_{k,j}^{[i]}, \tag{15}$$

and $\alpha_{k,j} \in [0, 1]$ is the weighting coefficient of $D_{k,j}$. Specifically, $\alpha_{k,j}$ represents the IT or EH requirement of $D_{k,j}$, and a tradeoff between IT and EH can be achieved by changing the value of $\alpha_{k,j}$. As shown in (13), the denominator of $M_{k,j}^C$ represents the total leakage interference of $D_{k,j}$ imposed on the other $K - 1$ clusters and the numerator of $M_{k,j}^C$ characterizes both the sum rate and the harvested power. Specifically, the first term of the numerator of $M_{k,j}^C$ represents the desired signal strength and the second term represents the harvested power from $D_{k,j}$. Based on the Rayleigh-Ritz theorem [32], the optimal value of $M_{k,j}^C$ is obtained by using the generalized eigenvalue decomposition (GEVD), yielding

$$M_{k,j}^{*C} = \lambda_1 (\mathbf{B}_{k,j}, \mathbf{A}_{k,j}), \tag{16}$$

where $\lambda_n (\mathbf{A}, \mathbf{B})$ denotes the n -th largest generalized eigenvalue of the matrix pair (\mathbf{A}, \mathbf{B}) . According to (16), $D_{k,j}$ computes the metric $M_{k,j}^C$ and feeds it back to CH_k . Then, CH_k selects a set of S nodes based on the S largest values of $M_{k,j}^C$ from all the nodes of the cluster. When the node selection is completed, CH_k broadcasts the scheduling information and the selected nodes calculate the transmit beamforming vector before conducting the uplink transmission. Similar to (13), the transmit beamforming vector of $D_{k,j}, j \in \Psi_k$, satisfies

$$\mathbf{v}_{k,j}^* = \arg \max_{\mathbf{v}_{k,j}} \frac{\mathbf{v}_{k,j}^H \mathbf{B}_{k,j}^* \mathbf{v}_{k,j}}{\mathbf{v}_{k,j}^H \mathbf{A}_{k,j} \mathbf{v}_{k,j}}, \tag{17}$$

where we have

$$\begin{aligned}
 \mathbf{B}_{k,j}^* &= \alpha_{k,j} \mathbf{H}_{k,j}^{[k]H} \mathbf{U}^{[k]} \mathbf{U}^{[k]H} \mathbf{H}_{k,j}^{[k]} \\
 &+ (1 - \alpha_{k,j}) \zeta \sum_{i \in \Phi_k} \mathbf{H}_{k,j}^{[k,i]H} \mathbf{H}_{k,j}^{[k,i]}. \tag{18}
 \end{aligned}$$

Then, for $D_{k,j}, j \in \Psi_k$, we obtain

$$\mathbf{v}_{k,j}^* = \mathbf{w}_1 (\mathbf{B}_{k,j}^*, \mathbf{A}_{k,j}), \tag{19}$$

where $\mathbf{w}_n (\mathbf{A}, \mathbf{B})$ represents the generalized eigenvector corresponding to $\lambda_n (\mathbf{A}, \mathbf{B})$.

Remark 1: It should be noted that for the scheduling metric design in (16) and the transmit beamforming design in (19) of the proposed C-ICPA-OIA scheme, we only consider the intra-cluster harvested power. The reason behind this is twofold. First, for a certain idle node, the inter-cluster harvested power is smaller than the intra-cluster harvested power due to the path loss. Second, it is not practical for each node to obtain the CSI from it to all the nodes in other clusters, and the CSI overheads increase very fast as the number of the nodes increase. Therefore, the objective of the proposed scheme is to achieve a tradeoff between facilitating efficient power transfer and acceptable CSI overheads.

The scheduling metric in (13) characterizes the sum rate performance and the harvested power simultaneously. As shown in our simulations of Section V, the proposed C-ICPA-OIA scheme is capable of achieving a better EH performance while maintaining a sum rate performance comparable to the conventional OIA scheme of [31]. However, by exploiting the characteristics of the multi-node transmission, the node scheduling strategy of C-ICPA-OIA can be further improved. As shown in (13), C-ICPA-OIA does not take the impact of ZF detection into account and only treats the overall signal strength within the RSS as a coarse description of the node's effective signal strength. In fact, the effective signal strength of each node after performing ZF detection is the value projected on a certain basis of the RSS, rather than the desired signal strength in the entire RSS. Therefore, the orthogonality among equivalent channel vectors of the nodes should be considered, and a refined ICPA-OIA scheme, namely the R-ICPA-OIA, is proposed in the next subsection.

For clarity, the implementation of the proposed C-ICPA-OIA scheme is summarized as Algorithm 1.

Algorithm 1 The Procedure of the C-ICPA-OIA Scheme

- 1) Initialization: Let $\Phi_k = [1, N]$, $\Psi_k = \emptyset$ and $l = 1$, where $k \in [1, K]$.
- 2) Node feedback: $D_{k,j}$ calculates the scheduling metric according to (16) and feeds it back to CH_k , $k \in [1, K]$, $j \in \Phi_k$.
- 3) Node selection: CH_k selects the node having the largest scheduling metric according to $\psi_k(l) = \arg \max_{j \in \Phi_k} M_{k,j}^C$, $k \in [1, K]$.
- 4) Update the selected node set: $\Phi_k = \Phi_k - \{\psi_k(l)\}$, $\Psi_k = \Psi_k \cup \{\psi_k(l)\}$, $k \in [1, K]$ and $l = l + 1$.
 - a) If $l \leq S$, go to Step 3.
 - b) Otherwise, go to Step 5.
- 5) Calculate beamforming vector: $D_{k,j}$ calculates its transmit beamforming vector using (19), $j \in \Psi_k$, $k \in [1, K]$.
- 6) Conduct IT and EH: The selected nodes carry out uplink transmission, the CHs detect the received signals and the unselected nodes harvest energy.

Furthermore, it is worth noting that, the C-ICPA-OIA scheme can be conducted in a distributed fashion. Assuming that all the nodes are synchronized to a common clock, such as the global positioning system (GPS) signal, a timer which lasts inverse-proportionally to $M_{k,j}^C$ is invoked. Explicitly, with the clock period T , the response time of the timer of $D_{k,j}$ can be defined as $\delta_{k,j} = T/M_{k,j}^C$. During each transmission block, each node calculates $\delta_{k,j}$ to trigger the timer. Upon receiving S feedback signals, the CH broadcasts an acknowledgement signal and the other nodes in the cluster keep silent. As a result, the first S time-out nodes will be included in Ψ_k .

B. THE PROPOSED SCHEME II: R-ICPA-OIA

In this subsection, we propose a R-ICPA-OIA scheme to more effectively characterize the intra-cluster performance. Each node has the values of S scheduling metrics and the s -th scheduling metric for $D_{k,j}$ is defined as

$$\begin{aligned}
 M_{k,j}^R(s) &= \frac{\alpha_{k,j} \left| \mathbf{u}_s^{[k]H} \mathbf{H}_{k,j}^{[k]} \mathbf{v}_{k,j} \right|^2 + (1 - \alpha_{k,j}) \zeta \sum_{i \neq j}^N \left\| \mathbf{H}_{k,j}^{[k,i]} \mathbf{v}_{k,j} \right\|^2}{\sum_{i=1, i \neq k}^K \left\| \mathbf{U}^{[i]H} \mathbf{H}_{k,j}^{[i]} \mathbf{v}_{k,j} \right\|^2} \\
 &= \frac{\mathbf{v}_{k,j}^H \mathbf{C}_{k,j}(s) \mathbf{v}_{k,j}}{\mathbf{v}_{k,j}^H \mathbf{A}_{k,j} \mathbf{v}_{k,j}}, \tag{20}
 \end{aligned}$$

where we have

$$\begin{aligned}
 \mathbf{C}_{k,j}(s) &= \alpha_{k,j} \mathbf{H}_{k,j}^{[k]H} \mathbf{u}_s^{[k]} \mathbf{u}_s^{[k]H} \mathbf{H}_{k,j}^{[k]} \\
 &\quad + (1 - \alpha_{k,j}) \sum_{i=1, i \neq j}^N \mathbf{H}_{k,j}^{[k,i]H} \mathbf{H}_{k,j}^{[k,i]}, \tag{21}
 \end{aligned}$$

$$\mathbf{A}_{k,j} = \sum_{i=1, i \neq k}^K \mathbf{H}_{k,j}^{[i]H} \mathbf{U}^{[i]} \mathbf{U}^{[i]H} \mathbf{H}_{k,j}^{[i]}. \tag{22}$$

As shown in (20), the first term in the numerator of $M_{k,j}^R$ quantifies the desired equivalent channel gain (ECG) projected on each dimension of the RSS. Keeping the EH performance of the C-ICPA-OIA scheme, the R-ICPA-OIA scheme further enhances the achievable sum rate by selecting the nodes whose equivalent channel vectors are quasi-orthogonal and by maximizing the desired signal strength which is projected on each dimension of the basis of the RSS. Similar to (16), the optimal value of $M_{k,j}^R(s)$ is obtained by using the GEVD, yielding

$$M_{k,j}^{*R}(s) = \lambda_1(\mathbf{C}_{k,j}(s), \mathbf{A}_{k,j}). \tag{23}$$

After $D_{k,j}$ computes and feeds the metric $M_{k,j}^{*R}$ back to CH_k , S nodes are selected at CH_k . Upon receiving the scheduling information from CH_k , the selected node $D_{k,\psi_k(s)}$ also gets its corresponding reference direction represented by $\mathbf{u}_s^{[k]}$. Then, the transmit beamforming vector of $D_{k,\psi_k(s)}$ can be calculated as

$$\mathbf{v}_{k,\psi_k(s)}^* = \arg \max_{\mathbf{v}_{k,j}} \frac{\mathbf{v}_{k,j}^H \mathbf{C}_{k,j}^*(s) \mathbf{v}_{k,j}}{\mathbf{v}_{k,j}^H \mathbf{A}_{k,j} \mathbf{v}_{k,j}}, \tag{24}$$

where we have

$$\begin{aligned}
 \mathbf{C}_{k,j}^*(s) &= \alpha_{k,j} \mathbf{H}_{k,j}^{[k]H} \mathbf{u}_s^{[k]} \mathbf{u}_s^{[k]H} \mathbf{H}_{k,j}^{[k]} \\
 &\quad + (1 - \alpha_{k,j}) \zeta \sum_{i \in \Phi_k} \mathbf{H}_{k,j}^{[k,i]H} \mathbf{H}_{k,j}^{[k,i]}. \tag{25}
 \end{aligned}$$

Then, for $D_{k,\psi_k(s)}$, the optimal transmit beamforming vector can be expressed as

$$\mathbf{v}_{k,\psi_k(s)}^* = \mathbf{w}_1(\mathbf{C}_{k,j}^*(s), \mathbf{A}_{k,j}). \tag{26}$$

Remark 2: Similar as the C-ICPA-OIA scheme, we only consider the intra-cluster harvested power for the scheduling metric design in (23) and the transmit beamforming design in (26), respectively. Due to the path loss, the amount of the harvested power at a certain unserved node is dominated by the intra-cluster power transfer. Moreover, the design principle of our scheme is to extend the basic idea of OIA, i.e., facilitating the information transmission with only local/partial CSI, to wireless power transfer.

The procedure of our R-ICPA-OIA scheme is summarized as Algorithm 2. Each node in each cluster calculates its S scheduling metrics and then feeds back to their home CH. Each CH uses the scheduling metrics to construct an $N \times S$ metric matrix. The columns of the matrix represent the orthonormal basis of the RSS. For a certain basis of the RSS, the node that is most aligned to the basis will be selected for uplink transmission.

C. FEEDBACK OVERHEAD AND COMPUTATIONAL COMPLEXITY

In this subsection, the feedback overhead and the computational complexity of the pair of ICPA-OIA schemes proposed are briefly analyzed. Furthermore, we compare our schemes with the traditional OIA schemes, i.e., the Min-LIF based

Algorithm 2 The Procedure of the R-ICPA-OIA Scheme

- 1) Initialization: Let $\Phi_k = [1, N]$, $\Psi_k = \emptyset$ and $l = 1$, where $k \in [1, K]$.
- 2) Node feedback: $D_{k,j}$ calculates S scheduling metrics using (23) and feeds them back to CH_k , $k \in [1, K]$, $j \in \Phi_k$.
- 3) Node selection: CH_k constructs an $N \times S$ metric matrix and search the matrix column by column. Specifically, CH_k selects the node with the largest scheduling metric according to $\psi_k(l) = \arg \max_{j \in \Phi_k} M_{k,j}^{*R}(l)$, $k \in [1, K]$.
- 4) Update the selected node set: $\Phi_k = \Phi_k - \{\psi_k(l)\}$, $\Psi_k = \Psi_k \cup \{\psi_k(l)\}$, $k \in [1, K]$ and $l = l + 1$.
 - a) If $l \leq S$, go to Step 3.
 - b) Otherwise, go to Step 5.
- 5) Calculate beamforming vector: $D_{k,j}$ calculates its transmit beamforming vector using (26), $j \in \Psi_k$, $k \in [1, K]$.
- 6) Conduct IT and EH: The selected nodes carry out uplink transmission, the CHs detect the received signals and the unselected nodes harvest energy.

OIA and the threshold based OIA, which do not take EH into account.

As pointed out in Section III-A, our C-ICPA-OIA scheme has the same amount of feedback overhead as the Min-LIF based OIA, since each node feeds back a single scalar value. For the threshold based OIA, the feedback overhead is quantified as $2S\varepsilon_1$ scalar values per node, where $\varepsilon_1 \in (0, 1)$ is the probability of the node satisfying the criteria in (10) and (11) for a certain receive beamforming vector, and it is determined by the system parameters, such as K, N, S and SNR. Additionally, as mentioned in Section III-B, the feedback overhead of our R-ICPA-OIA scheme is S scalar values. This feedback overhead can be further reduced by applying the threshold based limited feedback strategy. In what follows, the limited feedback version of our R-ICPA-OIA scheme is termed R-ICPA-LF-OIA. More specifically, a threshold η_{th} is introduced and each node in each cluster calculates its scheduling metrics. The value of η_{th} can be determined and broadcast to all nodes before the uplink transmission. As a result, the nodes whose LIF is higher than η_{th} , will not feed back the scheduling metrics. Therefore, the feedback overhead of our R-ICPA-OIA scheme reduces to $S\varepsilon_2$ scalar values per node, and $\varepsilon_2 \in (0, 1)$ represents that the probability of the node's LIF is lower than η_{th} . ε_2 is also determined by the system parameters, such as K, N and S . When the system parameters are given, and hence a proper value of η_{th} is determined, the R-ICPA-LF-OIA scheme is capable of imposing a feedback overhead comparable to that of the threshold based OIA scheme.

The computational complexity is characterized by the average number of floating-point operations (FLOPs)⁴ performed. The number of FLOPs for obtaining the scheduling

⁴Each addition, multiplication and division of real numbers cost one FLOP, respectively. Each multiplication of complex numbers costs six FLOPs.

metric and the transmit beamforming vector is counted, which is composed of two parts: calculating the scheduling metric and calculating the beamforming vector. We omit the analysis of the detection and decoding complexity after the equalization imposed on each CH, since it is the same for all the schemes considered. It is noted, by using the big O notation, we can subsume the computation with respect to the matrix multiplication, eigenvalue decomposition and etc. In the Min-LIF based scheme, the complexity for calculating the scheduling metric and the beamforming vector per node is $O(KSN_rN_t + KSN_t^2)$ [19]. Similarly, in the threshold based scheme, the computational complexity at each node is $O(KSN_r^2N_t + KSN_rN_t) + O(KS^2N_t^2) = O(KSN_r^2N_t + KS^2N_t^2)$. By comparison, in our C-ICPA-OIA scheme, the corresponding computational complexity becomes $O(SN_rN_t + SN_t^2) + O(NN_t^3) + O(KSN_rN_t + KSN_t^2) + O(N_t^3) = O(KSN_rN_t + KSN_t^2 + NN_t^3)$. Then, in our R-ICPA-OIA scheme, this complexity becomes $O(SN_rN_t + SN_t^2) + O(NSN_t^3) + O(KSN_rN_t + KSN_t^2) + O(SN_t^3) = O(NSN_t^3 + KSN_rN_t + KSN_t^2)$. For the sake of clarity, the feedback overhead and the computational complexity of the different OIA schemes considered are summarized in Table 1. Explicitly, we can see that the computational complexity of our C-ICPA-OIA and R-ICPA-OIA schemes is similar, albeit it is slightly higher than that of the conventional OIA schemes.

IV. PERFORMANCE ANALYSIS

In this section, the average harvested power and the average working time of the system are analyzed for demonstrating the effectiveness of the proposed schemes. To begin with, the average power harvested by the proposed two ICPA-OIA schemes is analyzed. In order to make a fair comparison, the average harvested power when using the conventional user/node scheduling schemes is also presented. Finally, the average working time of the proposed schemes is derived.

A. HARVESTED POWER

The average harvested power is defined as

$$E[\bar{Q}_{sum}] = \sum_{k=1}^K \sum_{n=1}^{N-S} E[Q_{k,\varphi_k(n)}]. \quad (27)$$

The average harvested power of the proposed two ICPA-OIA schemes as well as the the conventional node scheduling schemes can be presented as the following theorem.

Theorem 1: For the proposed C-ICPA-OIA and R-ICPA-OIA schemes, the average harvested power is lower bounded by

$$E[\bar{Q}_{sum}^{C-ICPA}] \geq E[\bar{Q}_{sum}^{Min-LIF}] = E[\bar{Q}_{sum}^{Threshold}], \quad (28)$$

$$E[\bar{Q}_{sum}^{R-ICPA}] \geq E[\bar{Q}_{sum}^{Min-LIF}] = E[\bar{Q}_{sum}^{Threshold}]. \quad (29)$$

Proof: Please see Appendix I. ■

TABLE 1. Feedback overhead and computational complexity of the different OIA schemes considered in terms of FLOPs.

| | Feedback overhead | Computational complexity |
|---------------------|--------------------------------------|------------------------------------|
| Min-LIF based OIA | 1 scheduling metrics | $O(KSN_r N_t + KSN_t^2)$ |
| Threshold based OIA | $2S\varepsilon_1$ scheduling metrics | $O(KSN_r^2 N_t + KSN_t^2)$ |
| C-ICPA-OIA | 1 scheduling metrics | $O(KSN_r N_t + KSN_t^2 + NN_t^3)$ |
| R-ICPA-OIA | S scheduling metrics | $O(NSN_t^3 + KSN_r N_t + KSN_t^2)$ |

Remark 3: It is noted that the average harvested power of the proposed two ICPA-OIA schemes outperform that of the conventional node scheduling schemes, which verifies the advantage of the proposed two ICPA-OIA schemes on the EH performance. Furthermore, the average harvested power of different OIA schemes also has impact on the working time of the system, which is analyzed in the following subsection.

B. WORKING TIME

Let us denote the initial power level at each node as E_0 . During each transmission block, the power consumed by the selected node is E_C and the power stored by the unselected node is E_S . According to the analysis in Section IV-A, E_S can be viewed as a constant. Without any loss of generality, we assume $E_C > E_S$. The working time $T_{k,j}$ of $D_{k,j}$ then satisfies the following criterion:

$$E_0 + (1 - P_{k,j}) E_S T_{k,j} = P_{k,j} E_C T_{k,j}, \tag{30}$$

where $P_{k,j}$ represents the probability of the event that $D_{k,j}$ is selected during the transmission block. The working time of the system is defined as

$$T = \min_{k,j} T_{k,j}. \tag{31}$$

From (30), we have

$$T_{k,j} = \frac{E_0}{(P_{k,j} E_C - (1 - P_{k,j}) E_S)}. \tag{32}$$

It is noted that the proposed two ICPA-OIA schemes and the conventional node scheduling schemes are essentially the opportunistic node selection schemes. For a certain node $D_{k,j}$, the average value of $P_{k,j}$ is the same in different node selection schemes. From Theorem 1, it is readily known that $E_S^{C-ICPA} \geq E_S^{Min-LIF} = E_S^{Threshold}$ and $E_S^{R-ICPA} \geq E_S^{Min-LIF} = E_S^{Threshold}$. Then, we have $T_{k,j}^{C-ICPA} \geq T_{k,j}^{Min-LIF} = T_{k,j}^{Threshold}$ and $T_{k,j}^{R-ICPA} \geq T_{k,j}^{Min-LIF} = T_{k,j}^{Threshold}$. Moreover, we can obtain $T^{C-ICPA} \geq T^{Min-LIF} = T^{Threshold}$ and $T^{R-ICPA} \geq T^{Min-LIF} = T^{Threshold}$. In Section V, numerical simulation results are provided to explicitly show the working time of different schemes considered.

V. NUMERICAL SIMULATIONS

In this section, we evaluate the performance of the proposed ICPA-OIA schemes with the aid of numerical simulations. The achievable sum rate of the system is chosen as the overall performance metric, which is defined in (4). The channel model used in the simulations is the same as the one described in Section II. Our simulation results are obtained via by 10^6 channel realizations. For the convenience of analysis,

ζ and $\alpha_{k,j}$ are set to 0.2 and 0.9, and $\beta_{k,j}^{[i]} = \beta_{k,j}^{[i,s]} = 1$, for $i = k$ and $\beta_{k,j}^{[i]} = \beta_{k,j}^{[i,s]} = 0.5$, for $i \neq k$ in the simulations.

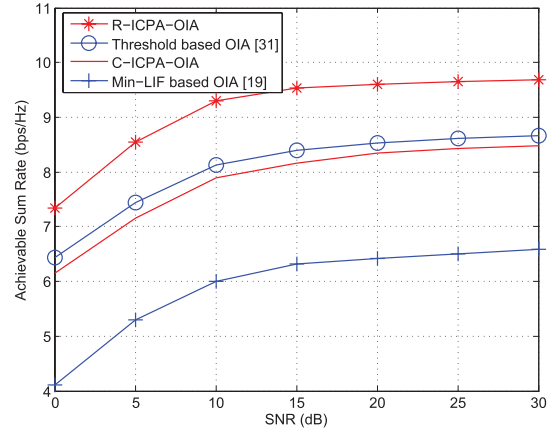


Fig. 2. The achievable sum rate versus the transmit SNR, where $K = 4$, $N_r = 4$, $N_t = 3$, $S = 3$, $N = 15$.

In Fig. 2, the achievable sum rate of the different OIA schemes considered is evaluated. We can see that the achievable sum rate of the proposed R-ICPA-OIA scheme is superior to the conventional OIA schemes across all SNR regimes. In addition, our C-ICPA-OIA scheme has a higher achievable sum rate than the Min-LIF based scheme that only considers the desired signal strength. Compared with the C-ICPA-OIA scheme, the R-ICPA-OIA scheme further mitigates the intra-cluster power loss and hence improves the achievable sum rate.

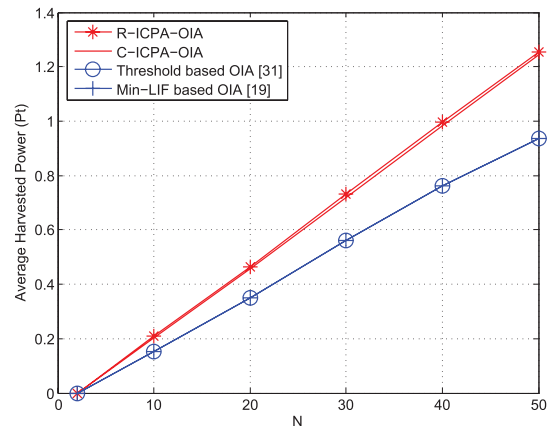


Fig. 3. The average harvested power versus the total number of nodes per cluster, where $K = 4$, $N_r = 4$, $N_t = 3$, $S = 2$.

Fig. 3 illustrates the average harvested power versus the total number of nodes per cluster. It is observed that our proposed schemes have a better energy harvesting performance than the Min-LIF scheme and the threshold based scheme.

Furthermore, the average harvested power in the R-ICPA-OIA scheme outperforms that of the C-ICPA-OIA scheme. Therefore, it is verified that the R-ICPA-OIA scheme is capable of achieving higher sum rate performance and energy harvesting performance.

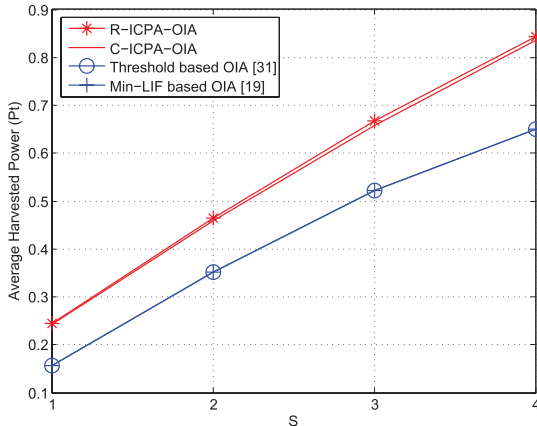


Fig. 4. The average harvested power versus the number of selected nodes per cluster, where $K = 4, N_r = 4, N_t = 3, N = 20$.

Fig. 4 shows the average harvested power versus the number of selected nodes per cluster. From Fig. 4, we can see that the proposed OIA schemes are capable of harvesting more power than the conventional OIA schemes. Moreover, the EH performance of the R-ICPA-OIA scheme is better than that of the C-ICPA-OIA scheme. The two traditional OIA schemes have the same EH performance because no EH metric is considered during the node selection.

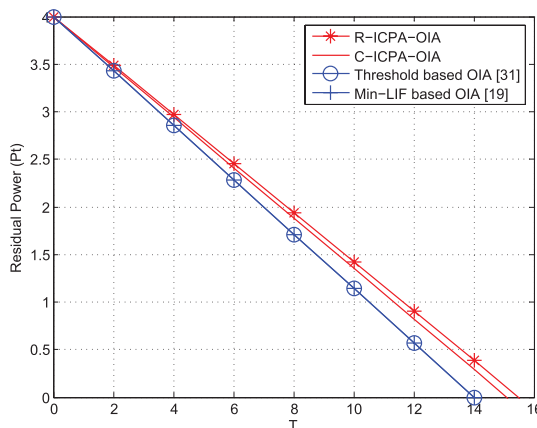


Fig. 5. The residual power of the node versus the working time, where $K = 4, N_r = 4, N_t = 3, S = 2, N = 20$.

In Fig. 5, we compare the residual power versus the working time of the node which first runs out in the network. According to the analysis in Section IV-B, it is assumed that $E_0 = 4P_t$ and $E_C = P_t$ in the simulation. As mentioned before, the two conventional OIA schemes have the same EH performance. Therefore, the working time of the two conventional OIA schemes is also the same and unsatisfactory. Meanwhile, the proposed two OIA schemes are capable of substantially increasing the working time of the node, which validates the effectiveness of the proposed schemes in the context of SWIPT.

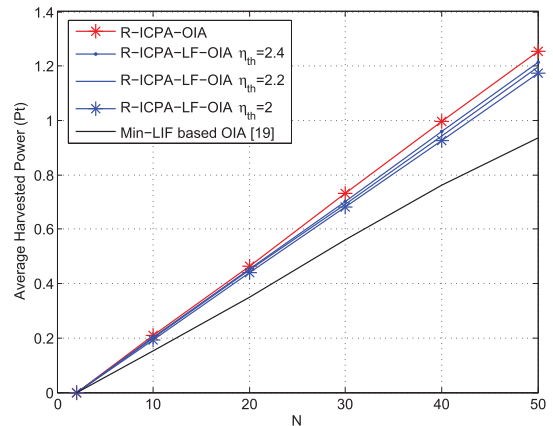


Fig. 6. The average harvested power in the R-ICPA-OIA scheme and the R-ICPA-LF-OIA scheme with different thresholds, $K = 4, N_r = 4, N_t = 3, S = 2$.

Finally, in Fig. 6 we investigate the impact of the threshold η_{th} on the average harvested power in the R-ICPA-LF-OIA scheme. It is observed that the R-ICPA-LF-OIA scheme harvests more energy when increasing η_{th} . Note that less feedback is needed when η_{th} is decreased. The suitable value of η_{th} in the proposed scheme depends on the specific system parameters. Therefore, in practical systems, the value of η_{th} can be carefully chosen according to the system configuration in order to achieve a tradeoff between the EH performance and the feedback overhead.

VI. CONCLUSIONS

In this paper, a pair of ICPA-OIA schemes are proposed for the K -cluster MIMO uplink SWIPT networks. In the proposed schemes, the scheduling metrics are carefully designed to characterize both the intra-cluster sum rate performance as well as the energy harvesting performance. Compared with the conventional OIA schemes, the proposed schemes effectively improve the achievable sum rate performance and the energy harvesting performance in the system. The theoretical analysis of the relationship between the achievable sum rate performance and the harvested power in the multi-cluster SWIPT systems will be carried out in our future work. Furthermore, in order to further improve the energy transfer efficiency, massive MIMO [33] as one promising technique in 5G can be integrated into the considered system, which is also an interesting topic.

APPENDIX I PROOF OF THEOREM 1

From (6), we have

$$\begin{aligned}
 Q_{k, \varphi_k(n)} &= \zeta P_t \sum_{p=1}^K \sum_{s=1}^S \left\| \tilde{\mathbf{h}}_{p, \psi_p(s)}^{[\varphi_k(n)]} \right\|^2 \\
 &= \zeta P_t \sum_{s=1}^S \left\| \tilde{\mathbf{h}}_{k, \psi_k(s)}^{[\varphi_k(n)]} \right\|^2 + \zeta P_t \sum_{p \neq k}^K \sum_{s=1}^S \left\| \tilde{\mathbf{h}}_{p, \psi_p(s)}^{[\varphi_k(n)]} \right\|^2,
 \end{aligned} \tag{33}$$

where the first term of (33) is the intra-cluster harvested energy and the second term of (33) is the inter-cluster harvested energy of $D_{k,\varphi_k(n)}$, respectively. Similarly, we can have

$$\begin{aligned} \bar{Q}_{\text{sum}} &= \zeta P_t \sum_{k=1}^K \sum_{n=1}^{N-S} \sum_{s=1}^S \left\| \check{\mathbf{h}}_{k,\psi_k(s)}^{[\varphi_k(n)]} \right\|^2 \\ &\quad + \zeta P_t \sum_{k=1}^K \sum_{n=1}^{N-S} \sum_{p \neq k}^K \sum_{s=1}^S \left\| \check{\mathbf{h}}_{p,\psi_p(s)}^{[\varphi_k(n)]} \right\|^2 \\ &= Q_{\text{sum}} + \tilde{Q}_{\text{sum}}. \end{aligned}$$

Recalling the proposed schemes in Section III, the scheduling metrics and the transmit beamforming vectors of the proposed schemes are designed with only the consideration of the intra-cluster power transfer. Thus, the merits of the proposed schemes are attributed to facilitating efficient intra-cluster power transfer, and for the inter-cluster energy harvesting, the proposed schemes obtain similar performance as the conventional OIA schemes. From the analysis above, it is noted that different OIA schemes have the same performance of \bar{Q}_{sum} . Next, we focus on the analysis of the average of the sum of intra-cluster harvested power, i.e., $E[Q_{\text{sum}}]$.

For the Min-LIF based scheme and the threshold based scheme, the node selection criteria have no impact on the EH performance, and the transmit beamforming vector $\mathbf{v}_{k,\psi_k(s)}$ of $D_{k,\psi_k(s)}$ is independent with the channel vector $\check{\mathbf{h}}_{k,\psi_k(s)}^{[k,\varphi_k(n)]}$, $n \in [1, N-S]$. We assume $\sigma_1^2 = \sigma_2^2 = 1$ and $\alpha_{k,j} = 0.5$. Then, we have

$$\begin{aligned} E[Q_{\text{sum}}^{\text{Min-LIF}}] &= E[Q_{\text{sum}}^{\text{Threshold}}] \\ &= \zeta P_t \sum_{k=1}^K \sum_{n=1}^{N-S} \sum_{s=1}^S E \left[\left\| \check{\mathbf{h}}_{k,\psi_k(s)}^{[\varphi_k(n)]} \right\|^2 \right] \\ &= K(N-S) \zeta P_t S \cdot E \left[\left\| \check{\mathbf{h}}_{k,\psi_k(s)}^{[\varphi_k(n)]} \right\|^2 \right] \\ &= 2K(N-S) \zeta P_t S N_t, \end{aligned} \quad (34)$$

where $\check{\mathbf{h}}_{k,\psi_k(s)}^{[\varphi_k(n)]}$ represents $\check{\mathbf{h}}_{k,\psi_k(s)}^{[k,\varphi_k(n)]}$ for simplicity, and $\left\| \check{\mathbf{h}}_{k,\psi_k(s)}^{[\varphi_k(n)]} \right\|^2$ obeys $\chi^2(2N_t)$ distribution and $\chi^2(k)$ represents the chi-square distribution with degrees of freedom of k .

In order to make the proof of (28) and (29) easy to understand, we introduce two intermediate variables, i.e., $E[Q_{\text{sum}}^{\text{C-ICPA-I}}]$ and $E[Q_{\text{sum}}^{\text{R-ICPA-I}}]$ in the proof. Specifically, in the first step, we decouple the node selection and transmit beamforming design in the proposed ICPA-OIA schemes. The random beamforming vector is adopted and the node selection procedure is based on Algorithm 1 and Algorithm 2. The corresponding harvested power of the proposed schemes are $E[Q_{\text{sum}}^{\text{C-ICPA-I}}]$ and $E[Q_{\text{sum}}^{\text{R-ICPA-I}}]$. In the second step, the harvested power of the proposed schemes, i.e., $E[Q_{\text{sum}}^{\text{C-ICPA-II}}]$ and $E[Q_{\text{sum}}^{\text{R-ICPA-II}}]$ are obtained.

Step I: For the proposed C-ICPA-OIA and R-ICPA-OIA schemes, without loss of generality, let us focus on the node selection in cluster 1. The random beamforming vector at

each node is adopted. We define $X_n = \left\| \check{\mathbf{h}}_{1,n}^{[1]} \right\|^2$, $Y_n = \sum_{k=2}^K \left\| \check{\mathbf{h}}_{1,n}^{[k]} \right\|^2$ and $Q_n = \sum_{s=1, s \neq n}^N \left\| \check{\mathbf{h}}_{1,n}^{[s]} \right\|^2$. Obviously, X_n obeys $\chi^2(2S)$, Y_n obeys $\chi^2(2(K-1)S)$ and Q_n obeys $\chi^2(2(N-1)N_t)$ distributions. The probability distribution functions (PDFs) of X_n , Y_n and Q_n are formulated as

$$f_{X_n}(x) = \frac{x^{S-1} e^{-\frac{x}{2}}}{2^S \Gamma(S)}, \quad (35)$$

$$f_{Y_n}(y) = \frac{y^{(K-1)S-1} e^{-\frac{y}{2}}}{2^{(K-1)S} \Gamma((K-1)S)}, \quad (36)$$

$$f_{Q_n}(q) = \frac{q^{(N-1)N_t-1} e^{-\frac{q}{2}}}{2^{(N-1)N_t} \Gamma((N-1)N_t)}, \quad (37)$$

where $\Gamma(x) = \int_0^\infty t^{x-1} e^{-t} dt$ is the Gamma function. Define $Z_n = \frac{X_n + Q_n}{Y_n}$ as the scheduling metric and $T_n = \frac{X_n/(2S)}{Y_n/(2(K-1)S)}$, $S_n = \frac{Q_n/(2(N-1)N_t)}{Y_n/(2(K-1)S)}$, $n \in [1, N]$. Then, T_n and S_n follow the F -distribution with degrees of freedom of $(2S, 2(K-1)S)$ and $(2(N-1)N_t, 2(K-1)S)$, respectively, and their cumulative distribution functions (CDFs) are given by

$$F_{T_n}(t) = \mathbb{I}_{\frac{t}{t+K-1}}(S, (K-1)S), \quad (38)$$

$$F_{S_n}(t) = \mathbb{I}_{\frac{t}{t+K-1}}((N-1)N_t, (K-1)S), \quad (39)$$

where $\mathbb{I}_t(a, b)$ is the regularized incomplete beta function which has the following properties:

$$\mathbb{I}_t(a, b) \leq \mathbb{I}_t(1, b) = 1 - (1-x)^b, \quad (40)$$

$$\mathbb{I}_t(a, b) \geq \mathbb{I}_t(a, 1) = x^a, \quad (41)$$

where $a, b \geq 1$. Since $Z_n = (K-1)T_n + \frac{(K-1)S}{(N-1)N_t} S_n$, the CDF of Z_n is formulated as

$$\begin{aligned} F_{Z_n}(z) &= F_{T_n}((K-1)z) + F_{S_n}\left(\frac{(K-1)S}{(N-1)N_t} z\right) \\ &= \mathbb{I}_{\frac{z}{z+1}}(S, (K-1)S) \\ &\quad + \mathbb{I}_{\frac{z}{z+(N-1)N_t}}(N_t, (K-1)N_t). \end{aligned} \quad (42)$$

According to (6), we have

$$\begin{aligned} E[Q_{\text{sum}}^{\text{C-ICPA-I}}] &= \zeta P_t \sum_{k=1}^K \sum_{n=1}^{N-S} \sum_{s=1}^S E \left[\left\| \check{\mathbf{h}}_{k,\psi_k(s)}^{[\varphi_k(n)]} \right\|^2 \right] \\ &= K(N-S) \zeta P_t S \cdot E[Q_{\psi_1(j)}], \end{aligned} \quad (43)$$

where $j \in [1, S]$. Similarly, the problem is studied in two cases.

For the case I: $j = 1$, the CDF of $Q_{\psi_1(1)}$, i.e., $F_{Q_1^*}(q)$ can be calculated as

$$\begin{aligned} F_{Q_1^*}(q) &= N \Pr\{Q_1 \leq q, \psi_1(1) = 1\} \\ &= N \Pr\left\{Q_1 \leq q, \frac{X_1 + Q_1}{Y_1} \geq Z_{\max, \bar{1}}\right\} \\ &= N \int_0^q qf_{Q_1}(q) F_{W_1}(q) dq, \end{aligned} \quad (44)$$

where $W_1 = Y_1 Z_{\max, \bar{1}}$ and $Z_{\max, \bar{1}} = \max_{n \in [2, N]} Z_n$. $f_{W_1}(w)$ and $F_{W_1}(w)$ are the PDF and CDF of W_1 , respectively and

$F_{W_1}(w)$ can be calculated as

$$\begin{aligned} F_{W_1}(w) &= \Pr \{ Y_1 Z_{\max, \bar{1}} \leq w \} \\ &= \int_0^\infty f_{Y_1}(y) \int_0^{\frac{w}{y}} f_{Z_{\max, \bar{1}}}(z) dz dy \\ &= \int_0^\infty f_{Y_1}(y) F_{Z_{\max, \bar{1}}}\left(\frac{w}{y}\right) dy, \end{aligned} \quad (45)$$

where $f_{Z_{\max, \bar{1}}}(z)$ and $F_{Z_{\max, \bar{1}}}(z)$ represent the PDF and CDF of $Z_{\max, \bar{1}}$, respectively. $F_{Z_{\max, \bar{1}}}(z)$ is given by

$$F_{Z_{\max, \bar{1}}}(z) = (F_{Z_n}(z))^{N-1}. \quad (46)$$

The PDF of $Q_{\psi_1(1)}$, i.e., $f_{Q_1^*}(q)$, is given by

$$f_{Q_1^*}(q) = Nq f_{Q_1}(q) F_{W_1}(q). \quad (47)$$

Based on (35), (36), (42), (45), (46) and (47), $E[Q_{\psi_1(1)}]$ is given by

$$\begin{aligned} E[Q_{\psi_1(1)}] &= \int_0^\infty Nq^2 f_{Q_1}(q) F_{W_1}(q) dq \\ &= \int_0^\infty Nq^2 f_{Q_1}(q) \int_0^\infty f_{Y_1}(y) F_{Z_{\max, \bar{1}}}\left(\frac{q}{y}\right) dy dq \\ &\stackrel{(a)}{\geq} \int_0^\infty Nq^2 f_{Q_1}(q) \int_0^\infty f_{Y_1}(y) \left(\frac{q}{q+y}\right)^\tau dy dq \\ &= \int_0^\infty Nq^2 \frac{q^{\tau-1} e^{-\frac{q}{2}}}{2^\tau \Gamma(\tau)} \int_0^\infty \frac{y^{\alpha-1} e^{-\frac{y}{2}}}{2^\alpha \Gamma(\alpha)} \left(\frac{q}{q+y}\right)^\tau dy dq \\ &\stackrel{(b)}{=} \int_0^\infty Nq^2 \frac{q^{\tau-1} e^{-\frac{q}{2}}}{2^\tau \Gamma(\tau)} \frac{q^{N_t N} e^{-\frac{q}{2}}}{2^{N_t N} \Gamma(N_t)} \\ &\quad \mathbb{U}\left(S(N-1), \tau - \alpha, \frac{q}{2}\right) dq \\ &\stackrel{(c)}{=} \frac{N}{2^\tau \Gamma(\tau)} (\theta_1 + \theta_2) \\ &\stackrel{(d)}{\geq} 2N_t, \end{aligned} \quad (48)$$

where $\theta_1 = \frac{\Gamma(S+1)\Gamma(N-1)\mathbb{F}(N_t, SN-1; S+N-1; 1)}{\Gamma(N+1)\Gamma(S)}$,

$\theta_2 = \frac{\Gamma(S+N_t+1)\Gamma(N)\mathbb{F}(S+N_t+1, SN+1; S+2; 1)}{\Gamma(N+1)\Gamma(S(N-1))\Gamma(S+1)}$, $\tau = N_t(N-1)$,

$\alpha = (K-1)S$, and $\mathbb{F}(a, b; c; z) = \sum_{n=0}^\infty \frac{(a)_n (b)_n}{(c)_n} \frac{z^n}{n!}$

is the hypergeometric function. (a) is due to (41). (b), (c) and (d) can be efficiently evaluated with software like MATLAB or Mathematica.

For the case II: $j = s$, $s \in [2, S]$, the CDF of $Q_{\psi_1(s)}$ is expressed as

$$\begin{aligned} F_{Q_s^*}(q) &= N \Pr \{ Q_1 \leq q, \psi_1(s) = 1 \} \\ &\stackrel{(e)}{\approx} (N-S) \Pr \{ Q_1 \leq q, \psi_1(1) = 1 \}, \end{aligned}$$

where (e) is due to the direct derivation from $F_{Q_s^*}(q)$ and the node with s -th largest scheduling metric among N nodes is considered as the node with largest scheduling metric among $N-S$ nodes. Then, we can replace N with $N-S$ in case I and the conclusion in case I still exists. To sum up, for the proposed C-ICPA-OIA scheme, we have $E[Q_{\text{sum}}^{\text{C-ICPA-I}}] \geq E[Q_{\text{sum}}^{\text{Min-LIF}}]$.

Step II: Compared with the random transmit beamforming vector, the GEVD based transmit beamforming vectors are adopted in our OIA schemes, and it is easy to obtain $E[Q_{\text{sum}}^{\text{C-ICPA}}] \geq E[Q_{\text{sum}}^{\text{C-ICPA-I}}]$.

To sum up, for the proposed C-ICPA-OIA scheme, we have $E[Q_{\text{sum}}^{\text{C-ICPA}}] \geq E[Q_{\text{sum}}^{\text{Min-LIF}}] = E[Q_{\text{sum}}^{\text{Threshold}}]$.

Following similar steps, we can prove that $E[Q_{\text{sum}}^{\text{R-ICPA}}] \geq E[Q_{\text{sum}}^{\text{Min-LIF}}]$.

Finally, we conclude that

$$\begin{aligned} E[\bar{Q}_{\text{sum}}^{\text{C-ICPA}}] &\geq E[\bar{Q}_{\text{sum}}^{\text{Min-LIF}}] = E[\bar{Q}_{\text{sum}}^{\text{Threshold}}], \\ E[\bar{Q}_{\text{sum}}^{\text{R-ICPA}}] &\geq E[\bar{Q}_{\text{sum}}^{\text{Min-LIF}}] = E[\bar{Q}_{\text{sum}}^{\text{Threshold}}]. \end{aligned}$$

The proof of Theorem 1 is finished.

REFERENCES

- [1] M. A. Maddah-Ali, A. S. Motahari, and A. K. Khandani, "Communication over MIMO X channels: Interference alignment, decomposition, and performance analysis," *IEEE Trans. Inf. Theory*, vol. 54, no. 8, pp. 3457–3470, Aug. 2008.
- [2] V. R. Cadambe and S. A. Jafar, "Interference alignment and degrees of freedom of the K -user interference channel," *IEEE Trans. Inf. Theory*, vol. 54, no. 8, pp. 3425–3441, Aug. 2008.
- [3] T. Gou and S. A. Jafar, "Degrees of freedom of the K -user $M \times N$ MIMO interference channel," *IEEE Trans. Inf. Theory*, vol. 56, no. 12, pp. 6040–6057, Dec. 2010.
- [4] C. Suh and D. Tse, "Interference alignment for cellular networks," in *Proc. 46th Annu. Allerton Conf. Commun., Control, Comput.*, Monticello, IL, USA, Sep. 2008, pp. 1037–1044.
- [5] K. T. K. Cheung, S. Yang, and L. Hanzo, "Distributed energy spectral efficiency optimization for partial/full interference alignment in multi-user multi-relay multi-cell MIMO systems," *IEEE Trans. Signal Process.*, vol. 64, no. 4, pp. 882–896, Feb. 2016.
- [6] R. T. Krishnamachari and M. K. Varanasi, "Interference alignment under limited feedback for MIMO interference channels," in *Proc. IEEE Int. Symp. Inf. Theory (ISIT)*, Austin, TX, USA, Jun. 2010, pp. 619–623.
- [7] O. El Ayach and R. W. Heath, "Interference alignment with analog channel state feedback," *IEEE Trans. Wireless Commun.*, vol. 11, no. 2, pp. 626–636, Feb. 2012.
- [8] D. Fang, S. Su, T. Lv, H. Gao, and W. Long, "Joint quantization strategy for uplink cooperative cellular interference alignment with limited feedback," in *Proc. IEEE Military Commun. Conf. (MILCOM)*, Orlando, FL, USA, Oct./Nov. 2012, pp. 1–5.
- [9] R. Zhou, T. Lv, W. Long, H. Gao, Y. Lu, and E. Liu, "Limited feedback schemes based on inter-cell interference alignment in two-cell interfering MIMO-MAC," in *Proc. IEEE Int. Conf. Commun. (ICC)*, Budapest, Hungary, Jun. 2013, pp. 5214–5218.
- [10] X. Chen and C. Yuen, "Performance analysis and optimization for interference alignment over MIMO interference channels with limited feedback," *IEEE Trans. Signal Process.*, vol. 62, no. 7, pp. 1785–1795, Apr. 2014.
- [11] H. Gao, T. Lv, D. Fang, S. Yang, and C. Yuen, "Limited feedback based interference alignment for interfering multi-access channels," *IEEE Commun. Lett.*, vol. 18, no. 4, pp. 540–543, Apr. 2014.
- [12] K. Gomadam, V. R. Cadambe, and S. A. Jafar, "A distributed numerical approach to interference alignment and applications to wireless interference networks," *IEEE Trans. Inf. Theory*, vol. 57, no. 6, pp. 3309–3322, Jun. 2011.
- [13] J. H. Lee and W. Choi, "On the achievable DoF and user scaling law of opportunistic interference alignment in 3-transmitter MIMO interference channels," *IEEE Trans. Wireless Commun.*, vol. 12, no. 6, pp. 2743–2753, Jun. 2013.
- [14] J. Leithon, C. Yuen, H. A. Suraweera, and H. Gao, "A new opportunistic interference alignment scheme and performance comparison of MIMO interference alignment with limited feedback," in *Proc. IEEE Globecom Workshops (GC Wkshps)*, Anaheim, CA, USA, Dec. 2012, pp. 1123–1127.
- [15] H. J. Yang, W.-Y. Shin, B. C. Jung, C. Suh, and A. Paulraj. (2013). "Opportunistic downlink interference alignment." [Online]. Available: <http://arxiv.org/abs/1312.7198>

[16] H. Liu, H. Gao, W. Long, and T. Lv, "A novel scheme for downlink opportunistic interference alignment," in *Proc. IEEE 21th Int. Conf. Telecommun. (ICT)*, Lisbon, Portugal, May 2014, pp. 231–235.

[17] B. C. Jung and W.-Y. Shin, "Opportunistic interference alignment for interference-limited cellular TDD uplink," *IEEE Commun. Lett.*, vol. 15, no. 2, pp. 148–150, Feb. 2011.

[18] B. C. Jung, D. Park, and W.-Y. Shin, "Opportunistic interference mitigation achieves optimal degrees-of-freedom in wireless multi-cell uplink networks," *IEEE Trans. Commun.*, vol. 60, no. 7, pp. 1935–1944, Jul. 2012.

[19] H. J. Yang, W. Shin, B. C. Jung, and A. Paulraj, "Opportunistic interference alignment for MIMO interfering multiple-access channels," *IEEE Trans. Wireless Commun.*, vol. 12, no. 5, pp. 2180–2192, May 2013.

[20] H. J. Yang, B. C. Jung, W.-Y. Shin, and A. Paulraj, "Codebook-based opportunistic interference alignment," *IEEE Trans. Signal Process.*, vol. 62, no. 6, pp. 2922–2937, Jun. 2014.

[21] H. Gao, J. Leithon, C. Yuen, and H. A. Suraweera, "New uplink opportunistic interference alignment: An active alignment approach," in *Proc. IEEE Wireless Commun. Netw. Conf. (WCNC)*, Shanghai, China, Apr. 2013, pp. 3066–3071.

[22] S.-H. Hur, B. C. Jung, and B. Rao, "Sum rate enhancement by maximizing SGINR in an opportunistic interference alignment scheme," in *Proc. 45th Asilomar Conf. Signals, Syst. Comput.*, Pacific Grove, CA, USA, Nov. 2011, pp. 354–358.

[23] H. J. Yang, W.-Y. Shin, B. C. Jung, and A. Paulraj, "A feasibility study on opportunistic interference alignment: Limited feedback and sum-rate enhancement," in *Proc. Conf. 46th Asilomar Conf. Signals, Syst. Comput. (ASILOMAR)*, Pacific Grove, CA, USA, Nov. 2012, pp. 1132–1136.

[24] Y. Ren, H. Gao, C. Yuen, T. Lv, and Y. Lu, "Intra-cell performance aware uplink opportunistic interference alignment," in *Proc. IEEE Wireless Commun. Netw. Conf. (WCNC)*, Istanbul, Turkey, Apr. 2014, pp. 526–531.

[25] I. Chih-Lin, C. Rowell, S. Han, Z. Xu, G. Li, and Z. Pan, "Toward green and soft: A 5G perspective," *IEEE Commun. Mag.*, vol. 52, no. 2, pp. 66–73, Feb. 2014.

[26] L. Wan, G. Han, L. Shu, and N. Feng, "The critical patients localization algorithm using sparse representation for mixed signals in emergency healthcare system," *IEEE Syst. J.*, vol. PP, no. 99, pp. 1–12, Apr. 2015, doi: 10.1109/JSYST.2015.2411745.

[27] N. Zhao, F. R. Yu, and V. C. M. Leung, "Opportunistic communications in interference alignment networks with wireless power transfer," *IEEE Wireless Commun.*, vol. 22, no. 1, pp. 88–95, Feb. 2015.

[28] N. Zhao, F. R. Yu, and V. C. M. Leung, "Wireless energy harvesting in interference alignment networks," *IEEE Commun. Mag.*, vol. 53, no. 6, pp. 72–78, Jun. 2015.

[29] R. Zhang and C. K. Ho, "MIMO broadcasting for simultaneous wireless information and power transfer," *IEEE Trans. Wireless Commun.*, vol. 12, no. 5, pp. 1989–2001, May 2013.

[30] K. Huang and E. Larsson, "Simultaneous information and power transfer for broadband wireless systems," *IEEE Trans. Signal Process.*, vol. 61, no. 23, pp. 5972–5986, Dec. 2013.

[31] B. C. Jung, S. M. Kim, H. J. Yang, and W.-Y. Shin, "On the joint design of beamforming and user scheduling in multi-cell MIMO uplink networks," in *Proc. IEEE Int. Symp. Pers., Indoor Mobile Radio Commun. (PIMRC)*, Washington, DC, USA, Sep. 2014, pp. 428–432.

[32] R. A. Horn and C. R. Johnson, *Matrix Analysis*. New York, NY, USA: Cambridge Univ. Press, 1990.

[33] L. Wan, G. Han, J. Jiang, J. Rodrigues, N. Feng, and T. Zhu, "DOA estimation for coherently distributed sources considering circular and noncircular signals in massive MIMO systems," *IEEE Syst. J.*, vol. PP, no. 99, pp. 1–9, Jul. 2015, doi: 10.1109/JSYST.2015.2445052.



TIEJUN LV (M'08–SM'12) received the M.S. and Ph.D. degrees in electronics engineering from the University of Electronic Science and Technology of China, Chengdu, China, in 1997 and 2000, respectively. From 2001 to 2003, he was a Post-Doctoral Fellow with Tsinghua University, Beijing, China. In 2005, he became a Full Professor with the School of Information and Communication Engineering, Beijing University of Posts and Telecommunications. From 2008 to 2009, he was a Visiting Professor with the Department of Electrical Engineering, Stanford University, Stanford, CA, USA. He has authored over 200 published technical papers on the physical layer of wireless mobile communications. His current research interests include signal processing, and communications theory and networking. He is a Senior Member of the Chinese Electronics Association. He was a recipient of the Program for New Century Excellent Talents in University Award from the Ministry of Education, China, in 2006.



HUI GAO (S'10–M'13) received the B.Eng. degree in information engineering and the Ph.D. degree in signal and information processing from the Beijing University of Posts and Telecommunications (BUPT), Beijing, China, in 2007 and 2012, respectively. From 2009 to 2012, he was a Research Assistant with the Wireless and Mobile Communications Technology Research and Development Center, Tsinghua University, Beijing. From 2012 to 2012, he was also a Research Assistant with the Singapore University of Technology and Design, Singapore, where he was a Post-Doctoral Researcher from 2012 to 2014. He is currently an Assistant Professor with the School of Information and Communication Engineering, BUPT. His research interests include massive multiple-input-multiple-output systems, cooperative communications, and ultrawideband wireless communications.



SHAOSHI YANG (S'09–M'13) received the B.Eng. degree in information engineering from the Beijing University of Posts and Telecommunications (BUPT), Beijing, China, in 2006, the Ph.D. degree in electronics and electrical engineering from the University of Southampton, U.K., in 2013, and the Ph.D. degree in signal and information processing from BUPT in 2014. He is currently a Post-Doctoral Research Fellow with the University of Southampton. From 2008 to 2009, he was an Intern Research Fellow with the Communications Technology Lab, Intel Labs, Beijing, where he focused on channel quality indicator channel design for mobile WiMAX (802.16m) standard. He has authored over 30 research papers on the IEEE journals and conferences. His research interests include MIMO signal processing, green radio, heterogeneous networks, cross-layer interference management, convex optimization and its applications. He has received a number of academic and research awards, including the prestigious Dean's Award for Early Career Research Excellence at University of Southampton, the PMC-Sierra Telecommunications Technology Paper Award at BUPT, the Electronics and Computer Science Scholarship of the University of Southampton, and the Best Ph.D. Thesis Award of BUPT. He is a member of IET and a Junior Member of the Isaac Newton Institute for Mathematical Sciences, Cambridge University, U.K. He also serves as a TPC Member of several major IEEE conferences, including the IEEE ICC, the GLOBECOM, the PIMRC, the ICCVE, the HPCC, and as a Guest Associate Editor of the IEEE JOURNAL ON SELECTED AREAS IN COMMUNICATIONS.



YUAN REN received the B.E. degree from the Beijing University of Posts and Telecommunications, Beijing, China, in 2010, where he is currently pursuing the Ph.D. degree with the School of Information and Communication Engineering. His current research interests include energy harvesting, cooperative communications, and interference alignment.